Important role of concomitant lymphangiogenesis for reparative angiogenesis in hind limb ischemia

Zhongyue Pu, M.D.[1]; Yuuki Shimizu, M.D., Ph.D.[1]; Kazuhito Tsuzuki, M.D.[1]; Junya Suzuki, M.D.[1]; Ryo Hayashida, M.D., Ph.D.[1]; Kazuhisa Kondo, M.D., Ph.D.[1]; Yusuke Fujikawa, M.D.[1]; Kazumasa Unno, M.D., Ph.D.[1]; Koji Ohashi, M.D., Ph.D.[1]; Mikito Takefuji, M.D., Ph.D.[1]; Yasuko K. Bando, M.D., Ph.D.[1]; Noriyuki Ouchi, M.D., Ph.D.[1]; John W. Calvert, Ph.D.[2]; Rei Shibata, M.D., Ph.D.[1]; Toyoaki Murohara, M.D., Ph.D.[1]

[1]Department of Cardiology, Nagoya University Graduate School of Medicine, Nagoya, Japan 466-8550

[2]Department of Surgery, Division of Cardiothoracic Surgery, Carlyle Fraser Heart Center, Emory University School of Medicine, Atlanta GA USA

Running title: Role of lymphangiogenesis in hind limb ischemia

Correspondence to:
Yuuki Shimizu, MD, PhD. or Toyoaki Murohara, MD, PhD.
Department of Cardiology, Nagoya University Graduate School of Medicine,
65 Tsurumai, Showa-ku, Nagoya, 466-8550 Japan.
Tel. +81-52-744-2147, Fax. +81-52-744-2138
E-mail: shimi123@med.nagoya-u.ac.jp or murohara@med.nagoya-u.ac.jp

Key Words: lymphangiogenesis; angiogenesis; tissue ischemia; adipose-derived regenerative cells; inflammation.

Subject codes: basic, Vascular Biology
Total word count: 7389 words
Total number of figures are 5 (and 11 supplemental figures).

TOC category-basic and translational

Abstract

Objective: Lymphatic vessels are distributed throughout the body and tightly collaborate with blood vessels to maintain tissue homeostasis. However, the functional roles of lymphangiogenesis in the process of reparative angiogenesis in ischemic tissues are largely unknown. Accordingly, we investigated potential roles of lymphangiogenesis using a mouse model of ischemia-induced angiogenesis.

Approach and Results: Male C57BL/6J mice were subjected to unilateral hind limb ischemia, in which not only angiogenesis but also lymphangiogenesis was induced. Next, the excessive and prolonged tissue edema model significantly deteriorated reparative angiogenesis and blood perfusion recovery in ischemic limbs. Finally, implantation of adipose-derived regenerative cells (ADRCs) augmented ischemia-induced lymphangiogenesis, which was accompanied by reduced tissue edema and inflammation, resulting in improving reparative angiogenesis and blood perfusion recovery. In addition, inhibition of lymphangiogenesis by MAZ51, a specific VEGF-R3 inhibitor, resulted in enhanced inflammatory cell infiltration, gene expression of TNFα, IL-1β, IL-6, TGFβ, angiostatin, vasohibin, and endostatin, and tissue edema, resulting in reduced angiogenesis.

Conclusions: The lymphatic system may have a clearance role of tissue edema and inflammation, which contribute to functional reparative angiogenesis in response to tissue ischemia. Modulation of lymphangiogenesis would become a novel therapeutic strategy for severe ischemic disease in addition to ordinary vascular intervention and therapeutic angiogenesis.

Abbreviations

ADRCs: adipose-derived regenerative cells
CLI: critical limb ischemia
DMEM: Dulbecco's modified Eagle's medium
EC: endothelial cell
FBS: fetal bovine serum
HLI: hind limb ischemia
LDPI: Laser Doppler perfusion imaging
LYVE-1: lymphatic vessel endothelial hyaluronan receptor 1
PAD: peripheral artery disease
POD: post-operative days
qPCR: quantitative Polymerase Chain Reaction
SVFs: stromal vascular fractions
TNF: Tumor Necrosis Factor
T2WI: T2 weighted Image
VEGFR3: vascular endothelial cell growth factor receptor-3
WBP: wound bed preparation

Introduction

Critical limb ischemia (CLI) represents a severe stage of peripheral artery disease (PAD) with pain at rest and/or ischemic ulcers or gangrene [1] [2]. CLI is a refractory condition that reduces the patients' quality of life (QOL), leading to poor prognosis [2]. Therefore, it is imperative to establish therapeutic strategies to prevent a progression to CLI in these patients [3].

Augmentation of angiogenesis by administration of pro-angiogenic cytokines or by transplantation of stem/progenitor cells is an additional therapeutic option for severe ischemic diseases [4] [5]. We previously demonstrated that implantation of autologous bone marrow mononuclear cells (BM-MNCs) significantly improved ischemic symptoms and angiogenesis in patients with CLI[6]. More recently, we have shown that implantation of autologous adipose-derived regenerative cells (ADRCs) promoted angiogenesis and healing of ischemic ulcers in similar patients[7].

In 2003, Schultz and co-workers first proposed the concept termed "wound bed preparation (WBP)" [8], which noted that excessive inflammation and edema of surrounding tissues are factors that hamper wound healing, and the management of WBP was a key to promote tissue regeneration and wound healing process [8] [9]. In this WBP, lymphatic vessels may function as the clearance system for extracellular fluid, inflammatory cytokines and cells [10] [11]. Thus, this system may be necessary and important for angiogenic recovery after severe ischemic insult. However, the role of lymphangiogenesis in a reparative angiogenesis in ischemic tissue is largely unknown.

Accordingly, we investigated the potential role of lymphangiogenesis in reparative angiogenesis using a well-established mouse model of hindlimb ischemia. We further examined the role of concomitant lymphangiogenesis during ADRC-mediated therapeutic angiogenesis.

Materials and Methods

Materials and Methods are available in the manuscript or online-only Supplemental File. The data, analytic methods, and study materials of this study are available from the corresponding author upon reasonable request.

Animal Care

All procedures of animal care and use in this study were approved by the Animal Ethics Review Board of the Nagoya University School of Medicine. Male C57BL/6J mice (age, 8 to 10 weeks) were purchased from Charles River Laboratories Japan Inc. (Kanagawa, Japan). We used the only male in present cell culture and in vivo studies as described in the ATVB Council Statement for considering "sex difference" as a biological variable[12]. We randomly assigned the animals to the experimental groups. All the mice were anesthetized with hydrochloric acid medetomidine (0.3 mg/kg), midazolam (4 mg/kg), and butorphanol tartrate (5 mg/kg) before surgical procedure as well as during Laser Doppler measurements of limb perfusion.

Mouse Model of Unilateral Hind Limb Ischemia

Unilateral hind limb ischemia (HLI) was induced in mice, by excising the femoral artery and attaching side branches in the left leg. The procedures were performed as previously described [13 14]. After HLI induction, all mice were randomly assigned either to the vehicle control group or to the treatment group. To investigate the effect of ADRC implantation-induced lymphangiogenesis on HLI, the mice were divided into two groups (n=5 in each group). The vehicle control group was administered with phosphate-buffered saline (PBS), while the ADRC group received ADRCs (1×10^6 cells) by intramuscular injection into 3 points of ischemic adductor muscles at postoperative day (POD) 1[13, 14]. In another experiment, to evaluate the effect of lymphangiogenesis inhibition on HLI, we postoperatively injected MAZ51 (Millipore Sigma) 10mg/kg[15, 16] into ischemic adductor muscles on days 3 and 5. In this experiment, the mice were divided into four groups (n=5 in each group) and separately received PBS+5%DMSO (same with MAZ51 dissolved concentration); ADRC+5%DMSO; MAZ51; and MAZ51+ADRC at each time point after HLI.

Laser Doppler Perfusion Imaging

We performed laser Doppler perfusion imaging (LDPI) using the LDPI system (Moor Instruments, Devon, UK) pre- and postoperatively at specific time points on days 7, 14, 21, and 28, to measure serial blood flow in both control and HLI groups with or without treatments [13]. The mice were maintained at a temperature of 37 °C during the imaging. Consecutive surveys were performed over the same area of interest (leg and foot) as the color-coded images. Quantitative values were expressed as a ratio of ischemic and non-ischemic limb[13, 14].

Mouse Model of Artificial Edema in HLI

To test if prolonged edema could have an adverse effect on angiogenesis, we created an artificial edema model with HLI. Mice with HLI were divided into a control group and experimental edema group which was administered phosphate-buffered saline (PBS) (300 μL/day) in a left adductor muscle once a day for 28 days (n=10-12). Then, laser Doppler blood perfusion image (LDPI) analyzer (Moor Instruments, Devon, UK) was used to evaluate the blood perfusion recovery after HLI induction, with or without artificial edema [13]. We simultaneously calculated the limb survival rate.

Isolation of Mouse ADRCs

ADRCs were isolated from the inguinal subcutaneous adipose tissue from different cohorts of mice specifically for the isolation. After surgically isolating the tissue completely, we digested it using 2 mg/mL type I collagenase (Wako) for 1 hour at 37 °C in an incubator. Mature adipocytes and stromal vascular fractions (SVFs) were separated by filtration (70 μm filter, BD Falcon, Ma) followed by centrifugation (1,200 rpm for 5 min) [13, 14]. SVFs were cultured in Dulbecco's modified Eagle's medium (DMEM) containing 10% fetal bovine serum (FBS) and antibiotic / antimycotic solution (Gibco). We labelled the adherent cells with ADRCs (P0). The 1st and 2nd passages of ADRCs were used in our experiments [13 14].

Immunofluorescence staining

The frozen sections were collected from the left adductor muscles from control mice or at specific time-points postoperatively. The sections of 6 μm thick were fixed in 4% paraformaldehyde, washed twice by PBS, and blocked using 1% BSA at room temperature for 1 h. We then incubated the sections with primary antibody CD31 mAb (1:200, BD Pharmingen) and lymphatic vessel endothelial hyaluronan receptor 1 (LYVE-1) Ab (4:1000, Acris) at 4 °C overnight, followed by incubation with secondary antibodies such as: Alexa-Fluor 488-conjugated anti-rabbit antibody (1:1000, Thermo Fisher Scientific) and Alexa-Fluor 594-conjugated anti-rat antibody (1:1000, Thermo Fisher Scientific) at room temperature for 1 hour [16-18]. The nuclei were identified with 4',6-diamidino-2-phenylindole (DAPI) (1:1000, Roche) and macrophages were detected by PE anti-mouse F4/80 mAb (1:1000, BioLegend) [17]. Images were

visualized on a BZ-X710 (KEYENCE) at ×20 magnification and we randomly selected 5 fields from one slide. Results were counted as the average positive cells per field using the Image J software (version 1.51) [16-18].

Real-Time Reverse Transcriptase Polymerase Chain Reaction Analysis

Total RNA was extracted using the miRNeasy Micro Kit (QIAGEN) from cultured ADRCs, human dermal lymphatic microvascular endothelial cells (HMVEC-dLys; Lonza), and frozen mice tissues, obtained from control mice and after HLI surgery using liquid nitrogen [19]. Reverse transcription was performed with 1μg total RNA using qPCR RT master mix kit (TOYOBO) [19]. The results of real-time RT-PCR for VEGF-C, VEGF-D, bFGF, VEGF-A, Adrenomedullin, HGF, TNF-α, IL-1β, IL-6, TGF-β, vasohibin, angiostatin, endostatin, and GAPDH were examined using 2μg of total cDNA from each sample on the Mx3000P Real-Time PCR System (Stratagene). SYBR Green was used according to manufacturer's instruction (Applied Biosystem), as a double-stranded DNA-specific dye. The ΔΔCT method was performed to quantify relative expression of target mRNAs normalized to that of GAPDH in each sample. The condition and primer sequences are listed in the online-only Data Supplement.

Quantification of tissue edema using Magnetic Resonance Imaging (MRI) and wet to dry ratio

We used both invasive and non-invasive ways of measurement techniques to quantify the tissue edema. The mice's bilateral legs were examined using a 1.5T whole body MRI scanner (MRS 3000 Benchtop MRI Systems; MR Solutions Ltd) in T2 weighted Image (T2WI) [20]. The extent of soft tissue edema was determined visually and measured quantitatively, changing from normal to ischemic legs through Δ area and Δ perimeter using Image J software. In addition, water content was also evaluated using the wet to dry weight ratio method [20]. In brief, the mice's left hind limbs were collected after being sacrificed by an overdose of anesthesia, followed by removing the skin and weighing it immediately to obtain wet weight. After incubating for 24 hours at 55 °C, the completely dried limbs were weighted again to assess the edema level. The wet to dry weight ratio was calculated by dividing the deference between wet and dry weight, using the dry weight [20].

Cell Culture in Normoxia and Hypoxia Condition

HMVEC-dLy and HMVEC-dBl were cultured in endothelial cell growth medium containing growth factors (EGM-2MV; Lonza) according to the manufacturer's instructions[16 18]. To stimulate hypoxic conditions, the cells were planted in 6-well plates and maintained in corresponding media until they were 80% confluent before transferring to an anaerobic jar. AnaeroPack® System (MGC) was used to create an environment with less than 0.1% of oxygen and more than 15% of CO_2 [21]. We immediately placed the paper sachet into the anaerobic jar containing the 6-plate inside and continually cultured the cells at 37 °C for another 24 hours.

Statistics

Results were expressed as mean±SEM. Unpaired Student's t-test was used to evaluate statistical significance between two groups; one-way ANOVA along with Tukey post hoc test was used for three or more groups. We also used two-way repeated-measures ANOVA (Bonferroni) to assess the changes over time. GraphPad Prism software version 8 (GraphPad Software Inc) was used. The normality of all data was verified with the Shapiro-Wilk's method by shapiro. test function in R (version 3.6.3). Data were also tested for equal variance. Values of $p<0.05$ denote statistical significance.

Results

Kinetics of Endogenous Lymphangiogenesis in the Setting of Ischemia-Induced Angiogenesis in a Hind limb

In an ischemic organ, endogenous angiogenesis is induced by hypoxic stimuli for protection against ischemic injury, minimizing tissue damage [22]. Conversely, although lymphatic revascularization plays an important role under pathological conditions in the functional recovery of damaged tissues [10], limited knowledge is available regarding the characterization and the adaptive change of lymphatic vessels in ischemic skeletal muscles. To address this issue, we examined whether endogenous lymphangiogenesis would be induced in HLI. First, we investigated the changes in the capillary lymphatic density and VEGF-C expression in HLI in the setting of blood perfusion recovery at post-operative days (POD) 0, 14, and 28. Immuno-staining was performed to detect vascular endothelial cells [CD31-positive cells (red)] and lymphatic endothelial cells [LYVE-1-positive cells (green)] [23] in HLI (Figure 1A). Our analysis revealed that

angiogenesis emerged after POD 3, whereas lymphangiogenesis emerged after POD 5. A remarkable change in terms of those the morphology and the size of lymphatic vessels could not be detected in ischemic adductor muscles. Both angiogenesis and endogenous lymphangiogenesis were induced in a time-dependent manner after ischemic injury in HLI (Figure 1B and C). Lymphangiogenesis in the ischemic gastrocnemius muscles was induced the same as that in the adductor muscles, too (Supplemental Figure 1). Further, the expression of VEGF-C was upregulated from POD 3 to 7 (compared with POD 0, 5.3-fold higher at POD 3, 13.4-fold higher at POD 5, and 6.8-fold higher at POD 7), and its peak was observed at POD 5 in response to ischemic injury in the skeletal muscles of our model (Figure 2D).

Establishment of New Mouse Model of Artificial Edema in HLI

While our results demonstrated that lymphatic revascularization in the skeletal muscle in HLI was induced during blood perfusion recovery, evidence on its role is currently lacking. Therefore, to determine the impact of functional lymphatic transport capacity loss in HLI, we created an excessive and prolonged tissue edema model mimicking lymphatic drainage deficiency in the local tissue of HLI (Figure 1D) and investigated its effect on the blood perfusion recovery. Magnetic resonance imaging (MRI) was used to evaluate the tissue edema, and water content was detected as white intensities on the T2W images (Figure 1E). The amputation-free survival rate was low in the artificial edema model in HLI (Figure 1F and G). Laser Doppler perfusion Images (LDPI) demonstrated that blood perfusion recovery was inhibited by the excessive and prolonged tissue edema compared with that in the control group (37±8% vs. 54±11% at POD 28) (Figure 1H and I).

Augmentation of Ischemia-Induced Lymphangiogenesis by ADRCs Implantation through Upregulation of VEGF-C

Although LDPI demonstrated that ADRC implantation in HLI could promote blood perfusion recovery (Figure 2A and B) with augmentation of angiogenesis (Figure 2E and F), it is still unknown whether ADRCs can concurrently induce lymphangiogenesis in HLI. Consequently, we investigated VEGF-C expression in ADRCs under a hypoxic condition both *in vitro* and in an ischemic hind limb tissue after ADRCs implantation to determine whether ADRCs have the potential ability to promote lymphangiogenesis in a paracrine manner. qPCR

demonstrated that hypoxic stimuli significantly increased VEGF-C expression in ADRCs compared with normoxia (Figure 2C) and that the VEGF-C expression in the ADRC-treated ischemic muscles was upregulated compared with than that in the PBS group (Figure 2D). In addition, immunofluorescence analysis with LYVE-1 staining revealed that the lymphatic capillary density increased with ADRC implantation in the ischemic limbs at POD 14 (LYVE-1-positive cells: 2.4-fold higher in the ADRC group than in the PBS group: Figure 2E and F). Therefore, these results indicated that ADRC implantation could promote ischemia-induced lymphangiogenesis in HLI with VEGF-C expression.

Ischemia-Induced Inflammation Clearance in Relation to Lymphangiogenesis Resulting in Suppression of the Expression of Anti-Angiogenic Cytokines

Given that excessive inflammation is one of the resistance factors in tissue regeneration and that the prolonged inflammation would induce tissue edema, which could also stunt the angiogenesis in HLI as demonstrated in Figure1C to H, we next evaluated the relationship between the formation of lymphatic vessels and the inflammatory responses in HLI[24, 25]. immunofluorescence analysis demonstrated that the number of macrophages was significantly upregulated in the response to the ischemic injury in the damaged tissue (8.9-fold increased: Figure 3A). Conversely, the accumulation of macrophages was improved by augmentation of lymphangiogenesis with ADRC implantation at POD 14 (Figure 3A and B). qPCR showed that the expressions of the inflammatory factors, such as TNF-a, IL1-β, IL6, and TGF-β, were upregulated in an ischemic tissue at POD14 after injury (TNF-a: 10-fold; IL1-β: 7-fold; IL-6: 11-fold; and TGF-β: 12-fold higher). However, these inflammatory reactions were attenuated in the ADRC group (Figure 3C).

We subsequently tested the expression of vasohibin, angiostatin, and endostatin, which are known as inflammation-inducible anti-angiogenic cytokines, and could suppress the neovascularization in several tissues[26, 27]. Figure 3D demonstrates that the expression of vasohibin, angiostatin, and endostatin in HLI was upregulated in the PBS group (vasohibin: 10.0-fold; angiostatin: 9.1-fold; endostatin 6.1-fold higher than that in the sham group). Conversely, these responses were partially canceled in the ADRC group compared with those in the PBS group (Figure 3D).

The inhibition of lymphangiogenesis partially canceled both of the endogenous and ADRCs-induced angiogenesis in HLI in the setting of the blood perfusion recovery

For further confirmation of the contribution of lymphangiogenesis on angiogenesis in HLI, we used MAZ51, which is a VEGFR-3 kinase inhibitor, to block lymphangiogenesis. MAZ51 inhibited not only the endogenous lymphangiogenesis (LYVE-1-positive cells at POD 14 after HLI induction: 10.2±1.1 per field in the PBS group vs. 4.7±0.5 per field in the MAZ51 group; $P<0.05$), but also ADRCs-induced lymphangiogenesis at POD 14 (LYVE-1-positive cells at POD 14 after HLI induction: 23.6±2.5 per field in the ADRC group vs. 15±1.3 per field in the ADRC+MAZ51 group; $P<0.01$) (Figure 4A and B). LDPI revealed that inhibition of lymphangiogenesis by MAZ51 deteriorated the blood perfusion recovery compared with that in the group with and without ADRCs implantation (56±7% in the PBS group at POD 28; 39±8% in the MAZ51 group at POD 28; 78±9% in the ADRC group at POD 28; and 68±8% in the ADRC+MAZ51 group at POD 28) (Figure 4C and D). Thereafter, we found that inhibition of lymphangiogenesis blocked endogenous ischemia-induced angiogenesis and suppressed the ADRC-induced angiogenesis in HLI (CD31-positive cells at POD 14: 100±9 per field in the PBS group; 50±6 per field in the MAZ51 group; 201±17 per field in the ADRC group; and 130±12 per field in the ADRC+MAZ51 group) (Figure 4E and F). Moreover, knockdown of VEGF-C in ADRC attenuated the lymphangiogenic effect of ADRC both in vitro and in vivo, too (Supplemental Figure 2 and 3), followed by the attenuation of angiogenesis and blood perfusion recovery.

We subsequently examined whether MAZ51 only blocked lymphangiogenesis in the lymphatic endothelial cells or also directly affected the blood endothelial cells in the ischemic hind limb. The functional assays for blood endothelial cells demonstrated that the treatment with MAZ51 in HMVEC-dBL did not interfere with the tube-like formation ability (Supplemental Fig. 4A through C) and the proliferative ability (Supplemental Figure 4D).

Improvement of Local Inflammation/Tissue Edema and Attenuation of Anti-Angiogenic Cytokines in HLI as the Potential Mechanisms of the Beneficial Effect of Lymphangiogenesis on Angiogenesis

In Figure 5A, the two upper panels show that edema was cleared in relation to lymphangiogenesis in the ADRC group compared with that in the PBS group

after limb ischemia induction. Conversely, the tissue edema worsened after inhibition of lymphangiogenesis by MAZ51, as shown in the two lower panels. Figure 5B and C demonstrate that both changes in the area and perimeter of the injured limbs decreased in the ADRC group compared with those in the control group. Conversely, inhibition of lymphangiogenesis aggravated those parameters and reversed the beneficial effects of ADRC implantation on at POD 14. The water content was also evaluated to assess the amount of edema using the wet-to-dry weight ratio in the limbs. Tissue edema was induced in HLI but was attenuated by the augmentation of lymphangiogenesis with ADRC implantation. Conversely, inhibition of lymphangiogenesis by MAZ51 worsened limb edema and eliminated the beneficial effect of ADRC implantation at POD 14 (wet-to-dry weight ratio: 0.05±0.01 in the sham group; 0.17±0.03 in the PBS group; 0.08±0.01 in the ADRC group; 0.27±0.05 in the MAZ51 group; and 0.14±0.02 in the ADRC+MAZ51 group) (Figure 5D). Moreover, the effect of ADRC implantation is attenuated by prolonged and excessive edema in terms of blood perfusion recovery in HLI (Supplemental Figure 5). As shown in Figure 5E and F, suppression of lymphangiogenesis by MAZ51 resulted in the accumulation of local macrophages in HLI (F4/80-positive cells: 74.2±4.9 per field in the PBS group; 30.8±3.8 per field in the ADRC group; 100.4±8.2 per field in the MAZ51 group; and 45.0±2.2 per field in the MAZ51+ADRC group). Additionally, lymphangiogenesis inhibition aggravated tissue inflammatory reactions of TNF-α, IL1-β, IL6 and TGF-β, and canceled the beneficial effect of ADRC implantation in these responses (Figure 5G). These results were finally followed by increased production of anti-angiogenic cytokines (angiostatin: 2.6-fold higher in the MAZ51 group than in the PBS group and 3.0-fold higher in the ADRC+MAZ51 group than in the ADRC group; vasohibin: 1.6-fold higher in the MAZ51 group than in the PBS group and 1.5-fold higher in the ADRC+MAZ51 group than in the ADRC group; endostatin: 2.7-fold higher in the MAZ51 group than in the PBS group and 4.0-fold higher in the ADRC+MAZ51 group than in the ADRC group) (Figure 5H). Endostatin, Vasohibin, and Angiostatin were co-stained by F4/80 positive cells, respectively (Supplemental Figure 6) in ischemic hind limbs.

Discussion

The major findings of the present study are as follows: (1) Endogenous lymphangiogenesis was induced in the setting of reparative angiogenesis in a limb ischemia model. (2) Severe tissue edema deteriorates blood perfusion recovery as well as limb salvage in HLI. (3) Local tissue edema and excessive inflammation were cleared in coordination with lymphangiogenesis in HLI. (4) Lymphangiogenesis inhibition has an adverse effect on blood perfusion recovery by increasing the expression of anti-angiogenic cytokines, as a result of prolonged inflammation. (5) Augmentation of lymphangiogenesis by ADRCs implantation contributed to the improved angiogenesis in HLI by the improved clearance of excessive tissue edema and inflammation.

Lymphatic vessels play a pivotal role in the lymphatic fluid transport, lipid absorption, and immune cells drainage from the interstitial space to venous circulation [11]. Under pathological conditions, the VEGF-C-VEGFR3 signaling functions as one of the pivotal pathways in lymphatic revascularization and modulates those lymphatic functions[10, 28]. Although lymphatic vessels are known to exist in the skeletal muscles[29] in the same manner as blood vessels, limited knowledge is available regarding their kinetics and role in HLI. Herein, we first demonstrated that endogenous lymphangiogenesis was induced during lymphatic rarefaction via ischemic injury, and VEGF-C expression was upregulated in a series of adaptive lymphangiogenesis accompanied with endogenous angiogenesis in the ischemic limb. Moreover, inhibition of VEGFR3 signaling by MAZ51, confirmatively suppressed lymphangiogenesis in HLI. Taken together, our data indicate that postnatal lymphangiogenesis in HLI was induced at least in part via the VEGF-C-VEGFR3 signaling pathway in the ischemic hind limb, regardless of whether angiogenesis and lymphangiogenesis were independent of each other[30].

Although the relationship between inflammation and angiogenesis is complicated and controversial in different settings, the continuous and excessive inflammatory responses, such as immune cell accumulation and pro-inflammatory cytokine release, eventually contribute to host injury [8]. For example, Tumor Necrosis Factor (TNF), as one of the major inflammatory mediators, induces multiple changes in endothelial cell (EC) gene expression and has also been reported to enhance angiogenesis by inducing an endothelial “tip cell” phenotype in short periods of stimulation (e.g., 2 to 3 days) [31]. Conversely, continuous TNF administration blocked endothelial cell proliferation

and migration *in vitro*[32-34] by decreasing the activity[35] and expression[36, 37] of vascular endothelial cell growth factor receptor-2 (VEGFR2). Another *in vivo* study reported that IL-10 suppressed the activity of pro-inflammatory M1 macrophage-related cytokines (IL-6 and TNF-α) and promoted the blood perfusion recovery in HLI[14]. As mentioned above, continuous pro-inflammatory reactions would be a resistance factor for angiogenesis at least in the subacute or chronic phase of ischemia, which could be a therapeutic target for ischemic diseases.

Tissue edema was caused by a bankruptcy of the balance between the lymphatic fluid supply and its drainage mainly through the lymphatic systems[25]. In pathological conditions, inflammation itself and subsequent many cytokines release in the regenerative tissues upregulate vascular permeability, that causes local tissue edema[38, 39]. In turn, the lymphatic system dysfunction, such after surgical resection and radiation as a cancer therapy, results in drainage capacity loss and thereby local tissue edema[25]. In the present study, our artificial edema model, mimicking excessive local tissue edema demonstrated that excessive and prolonged edema has an inhibitory effect on blood perfusion recovery in HLI. In addition, our data also revealed the therapeutic implications for the attenuation of the beneficial effect of ADRCs by the presence of severe edema. The evidence from the results may be important as in PAD patients with lymphatic dysfunction or limb edema, which might lower the efficacy of cell therapy. Therefore, proper control of tissue edema is indicated one of the key factors in managing Wound Bed Preparation (WBP), especially in the process of angiogenesis in HLI. A previous retrospective clinical study reported that multidisciplinary therapy, including WBP, was effective in improving mortality and the limb salvage rates in patients with CLI [40].

Our present study also found that the expression of some anti-angiogenic factors such as angiostatin, vasohibin, and endostatin, apparently increased in response to the accumulation of inflammatory cytokines after HLI induction; these reactions deteriorated by inhibition of lymphangiognenesis but were ameliorated by the augmentation of lymphangiogenesis. As an internal fragment of plasminogen, angiostatin can specifically inhibit endothelial cell proliferation[41-44]. It was reported to inhibit neovascularization in the chick CAM assay and the growth of metastases in a mouse tumor model[45]. As an isolated fragment of collagen XVIII, endostatin inhibits endothelial cell proliferation and angiogenesis in vivo[46-48]. Vasohibin-1 is stimulated by inflammatory cytokines

under a hypoxic condition[49 50]. It blocks neovascularization in the pathological conditions following vascular injury[51, 52]. Based on these theories, our findings can explain the mechanism underlying inhibition of angiogenesis by excessive inflammation via upregulation of anti-angiogenic cytokines in HLI. More importantly, the concept of elimination of prolonged severe inflammation and edema modulating lymphatic revascularization could help in the formation of a new mechanistic approach for HLI.

ADRCs are an easily obtainable cell populations from subcutaneous adipose tissue and considered to be useful cell sources, which have already been applied in clinical regenerative medicine[53]. Our initial study reported that ADRCs could secrete VEGF and SDF-1 in ischemic tissues, which can mobilize EPCs into ischemic tissue and consequently contribute to angiogenesis directly[13]. More recently, we also reported that the ADRCs produced PGE2, leading to angiogenesis via the release IL-10, which induced anti-inflammatory and anti-apoptotic effects[14]. In these manners, ADRCs can directly promote angiogenesis. Conversely, implantation of ADRCs in the lymphedema models was reported to be able to augment lymphangiogenesis, which accelerated the resolution of tissue edema and inflammation[17]. However, there has been no evidence on whether ADRC implantation could induce lymphangiogenesis in HLI and on its impact on ischemic repair to data. Our study is the first to demonstrate that ADRC implantation could induce functional lymphatic revascularization as therapeutic lymphangiogenesis in HLI and could contribute to angiogenesis and consequently blood perfusion recovery in an indirect manner (indicated as the schema in Supplemental figure 7). Interestingly, a direct contribution of the ADRCs via differentiation into lymphatic endothelial cells to neolymphangiogenesis is negligible (Supplemental figure 8). In addition, knockdown of VEGF-C in ADRC attenuated the lymphangiogenic effect of ADRC both in vitro and in vivo indicating that VEGF-C from ADRCs plays an important role, at least in part, in lymphangiogenesis.

In conclusion, lymphangiogenesis contributes to ischemia-induced angiogenesis by improving the surrounding resistance factors in HLI. Our findings could help in the formulation of a new mechanistic concept for therapeutic angiogenesis and might provide relevant information regarding additional novel therapeutic targets for CLI.

Acknowledgments
We are grateful to Yoko Inoue and Kanako Isono for their technical assistance.

Sources of Funding: This study was supported by grants (to Y.S. and to T.M.) from the Ministry of Education, Culture, Sports, Science and Technology of Japan; and a grant from Suzuken Memorial Foundation to Y.S.

Disclosures
None.

References
1. Kinlay S. Management of Critical Limb Ischemia. *Circ Cardiovasc Interv*. 2016;9:e001946.
2. Uccioli L, Meloni M, Izzo V, Giurato L, Merolla S and Gandini R. Critical limb ischemia: current challenges and future prospects. *Vasc Health Risk Manag*. 2018;14:63-74.
3. Laird JR, Singh GD and Armstrong EJ. Contemporary Management of Critical Limb Ischemia: The BEST Is Yet to Come. *J Am Coll Cardiol*. 2016;67:1914-6.
4. Gaspar D, Peixoto R, De Pieri A, Striegl B, Zeugolis DI and Raghunath M. Local pharmacological induction of angiogenesis: Drugs for cells and cells as drugs. *Adv Drug Deliv Rev*. 2019.
5. Kondo K, Yanishi K, Hayashida R, Shintani S, Shibata R, Murotani K, Ando M, Mizuno M, Fujiwara T, Murohara T, Matoba S and Investigators TF-uS. Long-Term Clinical Outcomes Survey of Bone Marrow-Derived Cell Therapy in Critical Limb Ischemia in Japan. *Circ J*. 2018;82:1168-1178.
6. Tateishi-Yuyama E, Matsubara H, Murohara T, Ikeda U, Shintani S, Masaki H, Amano K, Kishimoto Y, Yoshimoto K, Akashi H, Shimada K, Iwasaka T, Imaizumi T and Therapeutic Angiogenesis using Cell Transplantation Study I. Therapeutic angiogenesis for patients with limb ischaemia by autologous transplantation of bone-marrow cells: a pilot study and a randomised controlled trial. *Lancet*. 2002;360:427-35.
7. Katagiri T, Kondo K, Shibata R, Hayashida R, Shintani S, Yamaguchi S, Shimizu Y, Unno K, Kikuchi R, Kodama A, Takanari K, Kamei Y, Komori K and Murohara T. Therapeutic angiogenesis using autologous

adipose-derived regenerative cells in patients with critical limb ischaemia in Japan: a clinical pilot study. *Sci Rep*. 2020;10:16045.
8. Schultz GS, Sibbald RG, Falanga V, Ayello EA, Dowsett C, Harding K, Romanelli M, Stacey MC, Teot L and Vanscheidt W. Wound bed preparation: a systematic approach to wound management. *Wound Repair Regen*. 2003;11 Suppl 1:S1-28.
9. Nishijima A, Gosho M, Yoshida R, Yanagibayashi S, Takikawa M, Nishijima J, Sekido M and Yamamoto N. Effective wound bed preparation using maggot debridement therapy for patients with critical limb ischaemia. *J Wound Care*. 2017;26:483-489.
10. Zheng W, Aspelund A and Alitalo K. Lymphangiogenic factors, mechanisms, and applications. *J Clin Invest*. 2014;124:878-87.
11. Kerjaschki D. The lymphatic vasculature revisited. *J Clin Invest*. 2014;124:874-7.
12. Robinet P, Milewicz DM, Cassis LA, Leeper NJ, Lu HS and Smith JD. Consideration of Sex Differences in Design and Reporting of Experimental Arterial Pathology Studies-Statement From ATVB Council. *Arterioscler Thromb Vasc Biol*. 2018;38:292-303.
13. Kondo K, Shintani S, Shibata R, Murakami H, Murakami R, Imaizumi M, Kitagawa Y and Murohara T. Implantation of adipose-derived regenerative cells enhances ischemia-induced angiogenesis. *Arterioscler Thromb Vasc Biol*. 2009;29:61-6.
14. Hao C, Shintani S, Shimizu Y, Kondo K, Ishii M, Wu H and Murohara T. Therapeutic angiogenesis by autologous adipose-derived regenerative cells: comparison with bone marrow mononuclear cells. *Am J Physiol Heart Circ Physiol*. 2014;307:H869-79.
15. Benedito R, Rocha SF, Woeste M, Zamykal M, Radtke F, Casanovas O, Duarte A, Pytowski B and Adams RH. Notch-dependent VEGFR3 upregulation allows angiogenesis without VEGF-VEGFR2 signalling. *Nature*. 2012;484:110-4.
16. Shimizu Y, Polavarapu R, Eskla KL, Pantner Y, Nicholson CK, Ishii M, Brunnhoelzl D, Mauria R, Husain A, Naqvi N, Murohara T and Calvert JW. Impact of Lymphangiogenesis on Cardiac Remodeling After Ischemia and Reperfusion Injury. *J Am Heart Assoc*. 2018;7:e009565.
17. Shimizu Y, Shibata R, Shintani S, Ishii M and Murohara T. Therapeutic lymphangiogenesis with implantation of adipose-derived

regenerative cells. *J Am Heart Assoc*. 2012;1:e000877.
18. Shimizu Y, Shibata R, Ishii M, Ohashi K, Kambara T, Uemura Y, Yuasa D, Kataoka Y, Kihara S, Murohara T and Ouchi N. Adiponectin-mediated modulation of lymphatic vessel formation and lymphedema. *J Am Heart Assoc*. 2013;2:e000438.
19. Shumiya T, Shibata R, Shimizu Y, Ishii M, Kubota R, Shintani S and Murohara T. Evidence for the therapeutic potential of ex vivo expanded human endothelial progenitor cells using autologous serum. *Circ J*. 2010;74:1006-13.
20. Schmitz D, Bangen JM, Herborn CU, Husain B, Lendemans S, Flohe SB, Metz KA, Schade FU, Taeger G, Oberbeck JR, Kobbe P, Waydhas C and Flohe S. Isolated closed minor-muscle injury of the lower leg did not cause an obvious systemic immune response. *Inflamm Res*. 2010;59:141-9.
21. Ogura Y, Ouchi N, Ohashi K, Shibata R, Kataoka Y, Kambara T, Kito T, Maruyama S, Yuasa D, Matsuo K, Enomoto T, Uemura Y, Miyabe M, Ishii M, Yamamoto T, Shimizu Y, Walsh K and Murohara T. Therapeutic impact of follistatin-like 1 on myocardial ischemic injury in preclinical models. *Circulation*. 2012;126:1728-38.
22. Couffinhal T, Silver M, Zheng LP, Kearney M, Witzenbichler B and Isner JM. Mouse model of angiogenesis. *Am J Pathol*. 1998;152:1667-79.
23. Banerji S, Ni J, Wang SX, Clasper S, Su J, Tammi R, Jones M and Jackson DG. LYVE-1, a new homologue of the CD44 glycoprotein, is a lymph-specific receptor for hyaluronan. *J Cell Biol*. 1999;144:789-801.
24. Schwager S and Detmar M. Inflammation and Lymphatic Function. *Front Immunol*. 2019;10:308.
25. Santambrogio L. The Lymphatic Fluid. *Int Rev Cell Mol Biol*. 2018;337:111-133.
26. Watanabe K, Hasegawa Y, Yamashita H, Shimizu K, Ding Y, Abe M, Ohta H, Imagawa K, Hojo K, Maki H, Sonoda H and Sato Y. Vasohibin as an endothelium-derived negative feedback regulator of angiogenesis. *J Clin Invest*. 2004;114:898-907.
27. Sim BK, MacDonald NJ and Gubish ER. Angiostatin and endostatin: endogenous inhibitors of tumor growth. *Cancer Metastasis Rev*. 2000;19:181-90.
28. Joukov V, Pajusola K, Kaipainen A, Chilov D, Lahtinen I, Kukk E, Saksela O, Kalkkinen N and Alitalo K. A novel vascular endothelial growth

factor, VEGF-C, is a ligand for the Flt4 (VEGFR-3) and KDR (VEGFR-2) receptor tyrosine kinases. *EMBO J*. 1996;15:290-98.
29. Ji RC. Recent advances and new insights into muscular lymphangiogenesis in health and disease. *Life Sci*. 2018;211:261-269.
30. Witzenbichler B, Asahara T, Murohara T, Silver M, Spyridopoulos I, Magner M, Principe N, Kearney M, Hu JS and Isner JM. Vascular endothelial growth factor-C (VEGF-C/VEGF-2) promotes angiogenesis in the setting of tissue ischemia. *Am J Pathol*. 1998;153:381-94.
31. Sainson RC, Johnston DA, Chu HC, Holderfield MT, Nakatsu MN, Crampton SP, Davis J, Conn E and Hughes CC. TNF primes endothelial cells for angiogenic sprouting by inducing a tip cell phenotype. *Blood*. 2008;111:4997-5007.
32. Frater-Schroder M, Risau W, Hallmann R, Gautschi P and Bohlen P. Tumor necrosis factor type alpha, a potent inhibitor of endothelial cell growth in vitro, is angiogenic in vivo. *Proc Natl Acad Sci U S A*. 1987;84:5277-81.
33. Mano-Hirano Y, Sato N, Sawasaki Y, Haranaka K, Satomi N, Nariuchi H and Goto T. Inhibition of tumor-induced migration of bovine capillary endothelial cells by mouse and rabbit tumor necrosis factor. *J Natl Cancer Inst*. 1987;78:115-20.
34. Sato N, Goto T, Haranaka K, Satomi N, Nariuchi H, Mano-Hirano Y and Sawasaki Y. Actions of tumor necrosis factor on cultured vascular endothelial cells: morphologic modulation, growth inhibition, and cytotoxicity. *J Natl Cancer Inst*. 1986;76:1113-21.
35. Guo DQ, Wu LW, Dunbar JD, Ozes ON, Mayo LD, Kessler KM, Gustin JA, Baerwald MR, Jaffe EA, Warren RS and Donner DB. Tumor necrosis factor employs a protein-tyrosine phosphatase to inhibit activation of KDR and vascular endothelial cell growth factor-induced endothelial cell proliferation. *J Biol Chem*. 2000;275:11216-21.
36. Patterson C, Perrella MA, Endege WO, Yoshizumi M, Lee ME and Haber E. Downregulation of vascular endothelial growth factor receptors by tumor necrosis factor-alpha in cultured human vascular endothelial cells. *J Clin Invest*. 1996;98:490-6.
37. Menon C, Iyer M, Prabakaran I, Canter RJ, Lehr SC and Fraker DL. TNF-alpha downregulates vascular endothelial Flk-1 expression in human melanoma xenograft model. *Am J Physiol Heart Circ Physiol*.

2003;284:H317-29.
38. Marcos-Ramiro B, Garcia-Weber D and Millan J. TNF-induced endothelial barrier disruption: beyond actin and Rho. *Thromb Haemost*. 2014;112:1088-102.
39. Hippenstiel S, Krull M, Ikemann A, Risau W, Clauss M and Suttorp N. VEGF induces hyperpermeability by a direct action on endothelial cells. *Am J Physiol*. 1998;274:L678-84.
40. Hioki H, Miyashita Y, Miura T, Ebisawa S, Motoki H, Izawa A, Tomita T, Koyama J and Ikeda U. Prognostic improvement by multidisciplinary therapy in patients with critical limb ischemia. *Angiology*. 2015;66:187-94.
41. O'Reilly MS, Holmgren L, Shing Y, Chen C, Rosenthal RA, Moses M, Lane WS, Cao Y, Sage EH and Folkman J. Angiostatin: a novel angiogenesis inhibitor that mediates the suppression of metastases by a Lewis lung carcinoma. *Cell*. 1994;79:315-28.
42. Good DJ, Polverini PJ, Rastinejad F, Le Beau MM, Lemons RS, Frazier WA and Bouck NP. A tumor suppressor-dependent inhibitor of angiogenesis is immunologically and functionally indistinguishable from a fragment of thrombospondin. *Proc Natl Acad Sci U S A*. 1990;87:6624-8.
43. Rastinejad F, Polverini PJ and Bouck NP. Regulation of the activity of a new inhibitor of angiogenesis by a cancer suppressor gene. *Cell*. 1989;56:345-55.
44. Parangi S, O'Reilly M, Christofori G, Holmgren L, Grosfeld J, Folkman J and Hanahan D. Antiangiogenic therapy of transgenic mice impairs de novo tumor growth. *Proc Natl Acad Sci U S A*. 1996;93:2002-7.
45. Ribatti D. The Chick Embryo Chorioallantoic Membrane as an In Vivo Assay to Study Antiangiogenesis. *Pharmaceuticals (Basel)*. 2010;3:482-513.
46. O'Reilly MS, Boehm T, Shing Y, Fukai N, Vasios G, Lane WS, Flynn E, Birkhead JR, Olsen BR and Folkman J. Endostatin: an endogenous inhibitor of angiogenesis and tumor growth. *Cell*. 1997;88:277-85.
47. Marneros AG, She H, Zambarakji H, Hashizume H, Connolly EJ, Kim I, Gragoudas ES, Miller JW and Olsen BR. Endogenous endostatin inhibits choroidal neovascularization. *FASEB J*. 2007;21:3809-18.
48. Skovseth DK, Veuger MJ, Sorensen DR, De Angelis PM and Haraldsen G. Endostatin dramatically inhibits endothelial cell migration,

vascular morphogenesis, and perivascular cell recruitment in vivo. *Blood*. 2005;105:1044-51.
49. Miyake K, Nishida K, Kadota Y, Yamasaki H, Nasu T, Saitou D, Tanabe K, Sonoda H, Sato Y, Maeshima Y and Makino H. Inflammatory cytokine-induced expression of vasohibin-1 by rheumatoid synovial fibroblasts. *Acta Med Okayama*. 2009;63:349-58.
50. Zhou SY, Xie ZL, Xiao O, Yang XR, Heng BC and Sato Y. Inhibition of mouse alkali burn induced-corneal neovascularization by recombinant adenovirus encoding human vasohibin-1. *Mol Vis*. 2010;16:1389-98.
51. Shen J, Yang X, Xiao WH, Hackett SF, Sato Y and Campochiaro PA. Vasohibin is up-regulated by VEGF in the retina and suppresses VEGF receptor 2 and retinal neovascularization. *FASEB J*. 2006;20:723-5.
52. Yamashita H, Abe M, Watanabe K, Shimizu K, Moriya T, Sato A, Satomi S, Ohta H, Sonoda H and Sato Y. Vasohibin prevents arterial neointimal formation through angiogenesis inhibition. *Biochem Biophys Res Commun*. 2006;345:919-25.
53. Shimizu Y, Calvert JW and Murohara T. Adipose-Derived Regenerative Cells for Cardiovascular Regeneration--A Novel Therapy for the Cardiac Conduction System. *Circ J*. 2015;79:2555-6.

Highlights

1. The lymphatic system in an ischemic limb has a compensatory function for inflammation and interstitial edema, which could contribute to enhanced angiogenesis.
2. ADRC implantation can promote ischemia-induced lymphangiogenesis in an ischemic limb.
3. Modulation of lymphangiogenesis would be a novel therapeutic target for PAD in addition to the ordinary therapeutic angiogenesis.

Figure legends

Figure 1. Endogenous lymphangiogenesis was induced in HLI and the excessive and prolonged edema stunts the blood perfusion recovery. (A) Representative fluorescence microscopy images of ischemic adductor muscle sections of sham or at postoperative day 0, 3, 5, 7, 14, and 28 stained with anti-CD-31 (Red) and anti-LYVE-1 (Green) antibody (×400). Scale bar=50 μm. (B) (C) Quantitative analysis of the number of CD-31 positive cells and that of LYVE-1 positive cells per field in the different time points under an ischemic condition of hind limb. Values are mean ± SEM (n=5). *P<0.05, **P<0.01, ***P<0.001 vs. sham by one-way ANOVA and Tukey's post hoc tests. (D) Representative images of newly established mouse model of artificial edema in HLI. (E) MRI T2W image showed the edema extent in an artificial edema model as a high intensity area in a left adductor muscle. (F) (G) Amputation free survival rate in ischemic limbs is evaluated by comparing control and edema group for up to 28 days after HLI induction. *P<0.05 vs. Control, analyzed with Kaplan Meyer estimators and Log-rank (Mantel-Cox) test (n=10-12). (H) Representative Laser Doppler blood perfusion Images (LDPI) and (I) the quantification of a LDPI ratio (ischemic/non-ischemic). Data are mean ± SEM (n=5). *P<0.05 vs. Control, by two-way ANOVA and Bonferroni post hoc tests.

Figure 2. ADRC implantation promoted lymphangiogenesis through the VEGF-C expression in the setting of blood perfusion recovery in HLI. (A) Representative LDP images and (B) summary of LDPI ratio (ischemic/non-ischemic) in the setting of blood perfusion recovery with or without ADRCs implantation. Data are mean ± SEM (n=5). *P<0.05, by two-way ANOVA and Bonferroni post hoc tests. (C) The expression of VEGF-C in the isolated ADRCs under the hypoxia condition. (D) mRNA levels of VEGF-C in the samples collected from PBS injected or ADRC-transplanted ischemic muscles at post-HLI day 0, 3, 5 and 7. Data are mean ± SEM (n=5). *P<0.05, by two-way ANOVA and Bonferroni post hoc tests., #P<0.05 vs. Sham, †p<0.05 vs. Sham, by one-way ANOVA and Tukey's post hoc tests. (E) Immuno-staining with anti-CD-31 (Red) and LYVE-1 (Green) in sham, PBS or ADRCs implantation group and (F) quantitative analysis of CD31 positive cells and LYVE-1 positive cells for each group in an ischemic limb at day 14 (×400). Scale bar=50μm. Data are mean ± SEM (n=5). *P<0.05 vs. sham, #P<0.05 vs. PBS, by one-way ANOVA and Tukey's post hoc tests.

Figure 3. **Local inflammation in HLI was improved coordinating with lymphangiogenesis by ADRCs, resulting in suppressed the expression of anti-angiogenic cytokines.** (A) Immuno-staining with anti-F4/80 (Red) for the ischemic tissue sections from sham, HLI+PBS treated or HLI+ADRC implanted mice to denote the accumulating macrophages in HLI at postoperative day 14 (×400). Scale bar=50 μm. (B) Quantitative analysis of the number of macrophages in the response to the ischemic injury in HLI with or without augmentation of lymphangiogenesis by ADRCs treatment. (C)The expressions of mRNA TNF-α, IL-1β, IL-6, and TGF-β in HLI with or without augmentation of lymphangiogenesis by ADRCs. (D) The expressions of vasohibin, angiostatin and endostatin after ischemic injury at day 14 post-operation. Data are mean ± SEM (n=5). *P<0.05, **P<0.01, ***P<0.001 vs. Sham, #P<0.05, ##P<0.01, ###P<0.001 vs. PBS, by one-way ANOVA and Tukey's post hoc tests.

Figure 4. The inhibition of lymphangiogenesis partially eliminated both the endogenous angiogenesis and the ADRCs-induced angiogenesis in HLI. (A) Representative images of the ischemic tissue sections in PBS, ADRC implantation, MAZ51 (VEGFR-3 inhibitor) treatment or ADRC+MAZ51 treatment groups at day 14 post-operation, stained with anti-LYVE-1 (Green) to denote lymphatic endothelial cells (LECs) and DAPI (Blue) (×400). Scale bar=50 μm. (B) Quantitative analysis of LYVE-1 positive cells in HLI by MAZ51 treatment. *P<0.05, **P<0.01 vs. PBS, ##P<0.01 vs. ADRC, analyzed by one-way ANOVA and Tukey's post hoc tests. (C) Representative images and (D) summary of LDPI ratio (ischemic/non-ischemic) by lymphangiogenesis inhibition with MAZ51. Data are mean ± SEM (n=5). *P<0.05 vs. PBS, #P<0.05 vs. ADRC, analyzed using two-way ANOVA and Bonferroni post hoc tests. (E) Immuno-staining with anti-CD-31 (Red) to detect blood endothelial cells (×400). Scale bar=50 μm. (F) Quantitative analysis of CD31 positive cells in HLI by the inhibition of lymphangiogenesis with MAZ51. Data are mean ± SEM (n=5). *P<0.05 vs. PBS, #P<0.05 vs. ADRC, by one-way ANOVA and Tukey's post hoc tests.

Figure 5. Suppression of lymphangiogenesis has adverse effects on the clearance of local inflammation/tissue edema and upregulates the anti-angiogenic cytokines in HLI. (A) Magnetic resonance imaging (MRI) by T2W signal to detect the tissue edema as the high intensity (white color). (B) Δ

Area and (C) Δ Perimeter are used as a measure of the limb swelling in HLI. (D) Water contents in HLI is also evaluated using wet to dry ratio (wet:dry). Samples were collected from ischemic adductor tissues in SHAM, PBS, ADRC implantation, MAZ51 treatment or ADRC plus MAZ51 treatment groups. (E) Representative images and (F) summary of the number of macrophages per field stained by anti-F4/80 (×400). Scale bar=50 μm. (G) The expressions of mRNA TNF-α, IL-1β, IL-6, and TGF-β in the case of the anti-lymphangiogenesis by MAZ51 in HLI. (H) The expressions of vasohibin, angiostatin and endostatin in HLI with or without MAZ51 treatment by qPCR. Data are mean ± SEM (n=5). *P<0.05, **P<0.01, ***P<0.001 vs. PBS, #P<0.05, ##P<0.01, ###P<0.001 vs. ADRC, **†††** P<0.001 vs. Sham, by one-way ANOVA and Tukey's post hoc tests. A+M, ADRC+MAZ51.

Figure 1

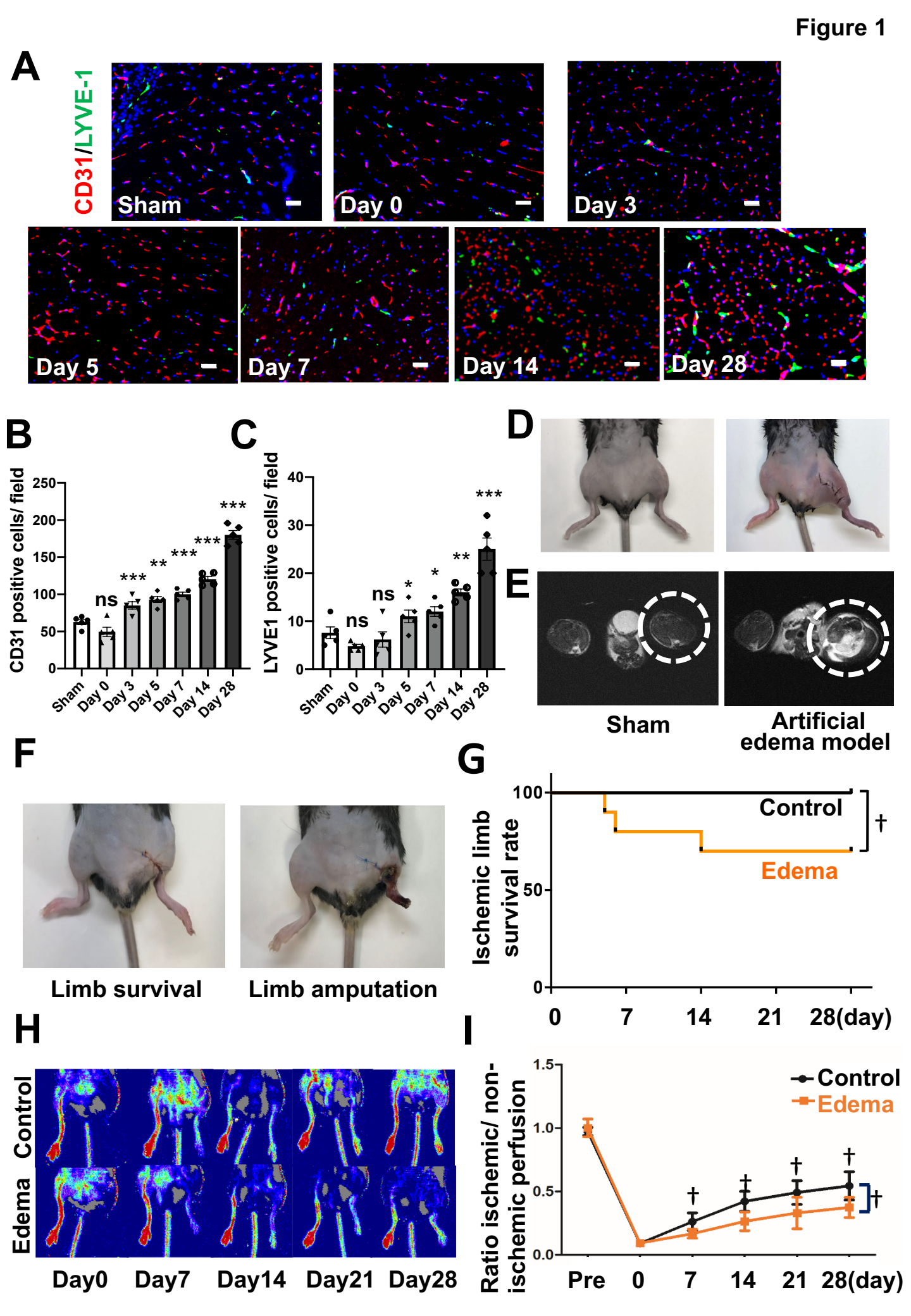
A
CD31/LYVE-1
Sham
Day 0
Day 3
Day 5
Day 7
Day 14
Day 28
B
CD31 positive cells/ field
ns
***
**
*
C
LYVE1 positive cells/ field
D
E
Sham
Artificial edema model
F
Limb survival
Limb amputation
G
Ischemic limb survival rate
Control
Edema
†
0
7
14
21
28(day)
H
Control
Edema
Day0
Day7
Day14
Day21
Day28
I
Ratio ischemic/ non-ischemic perfusion
Control
Edema
Pre
0
7
14
21
28(day)

Figure 2

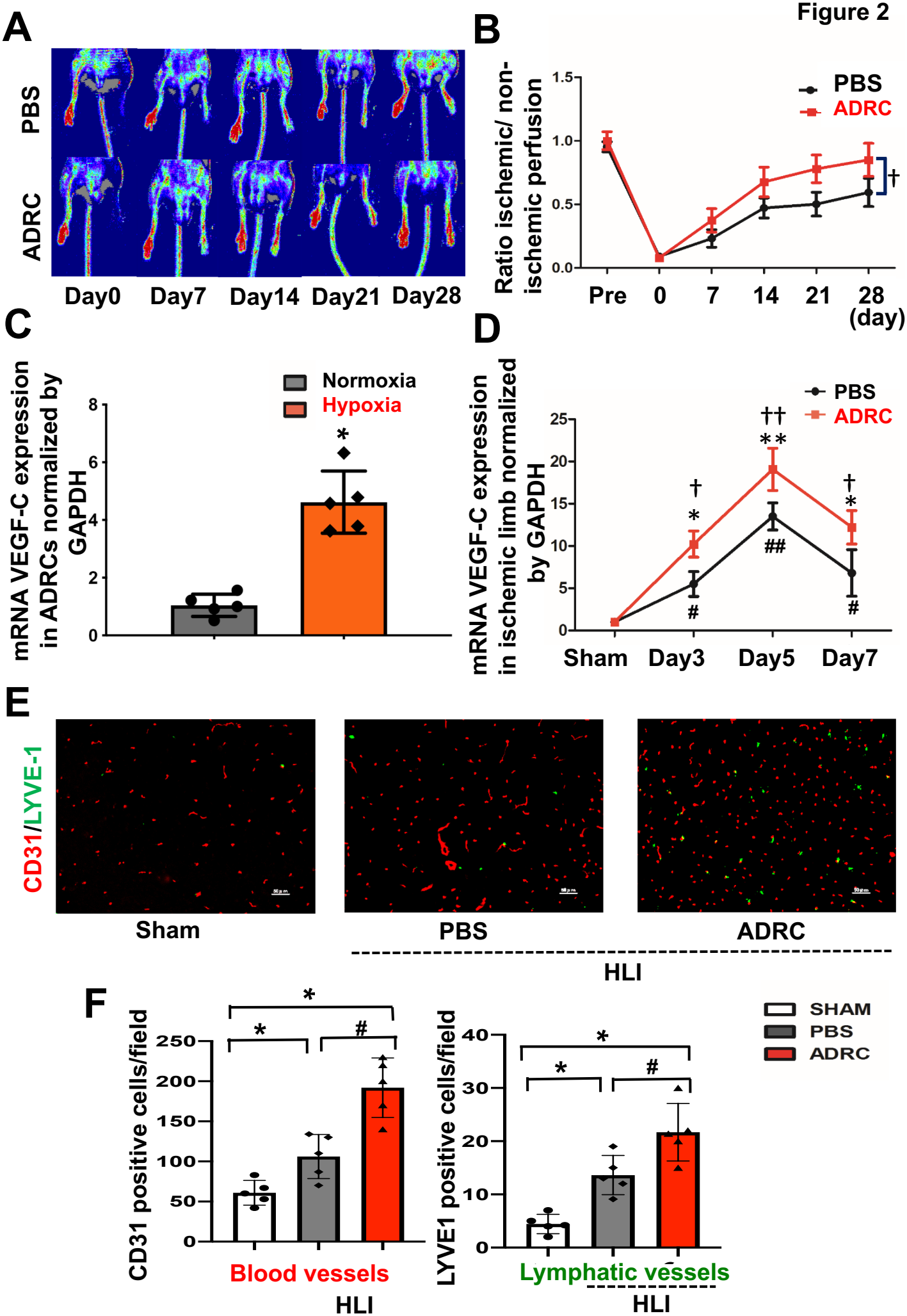
A
PBS
ADRC
Day0
Day7
Day14
Day21
Day28
B
Ratio ischemic/ non-ischemic perfusion
PBS
ADRC
Pre
0
7
14
21
28
(day)
C
mRNA VEGF-C expression in ADRCs normalized by GAPDH
Normoxia
Hypoxia
D
mRNA VEGF-C expression in ischemic limb normalized by GAPDH
PBS
ADRC
Sham
Day3
Day5
Day7
E
CD31/LYVE-1
Sham
PBS
ADRC
HLI
F
CD31 positive cells/field
Blood vessels
HLI
LYVE1 positive cells/field
Lymphatic vessels
HLI
SHAM
PBS
ADRC

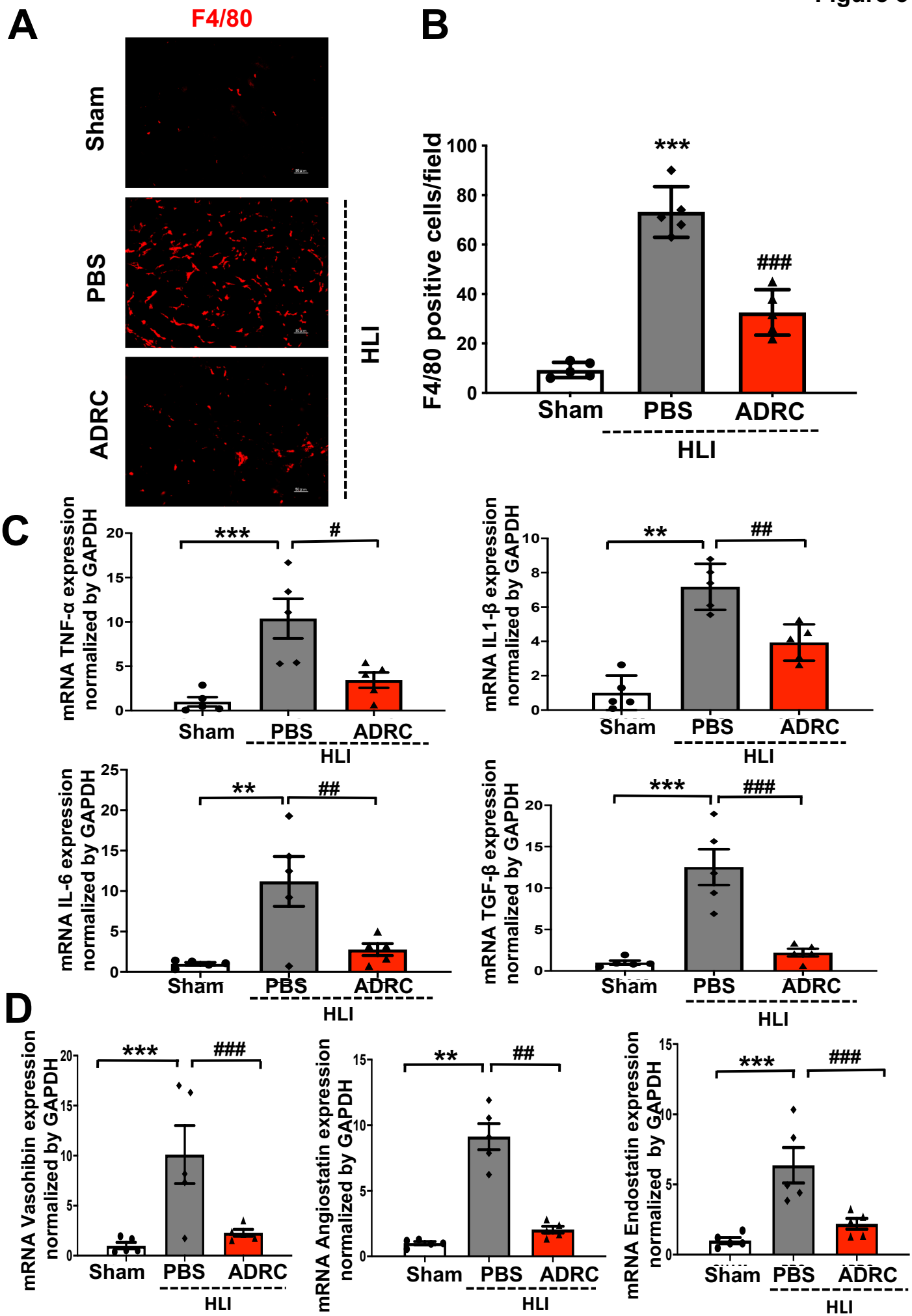
A
F4/80
Sham
PBS
ADRC
HLI
B
F4/80 positive cells/field
***
###
Sham
PBS
ADRC
HLI
C
mRNA TNF-α expression normalized by GAPDH
***
#
mRNA IL1-β expression normalized by GAPDH
**
##
mRNA IL-6 expression normalized by GAPDH
**
##
mRNA TGF-β expression normalized by GAPDH
***
###
D
mRNA Vasohibin expression normalized by GAPDH
***
###
mRNA Angiostatin expression normalized by GAPDH
**
##
mRNA Endostatin expression normalized by GAPDH
***
###

Figure 4

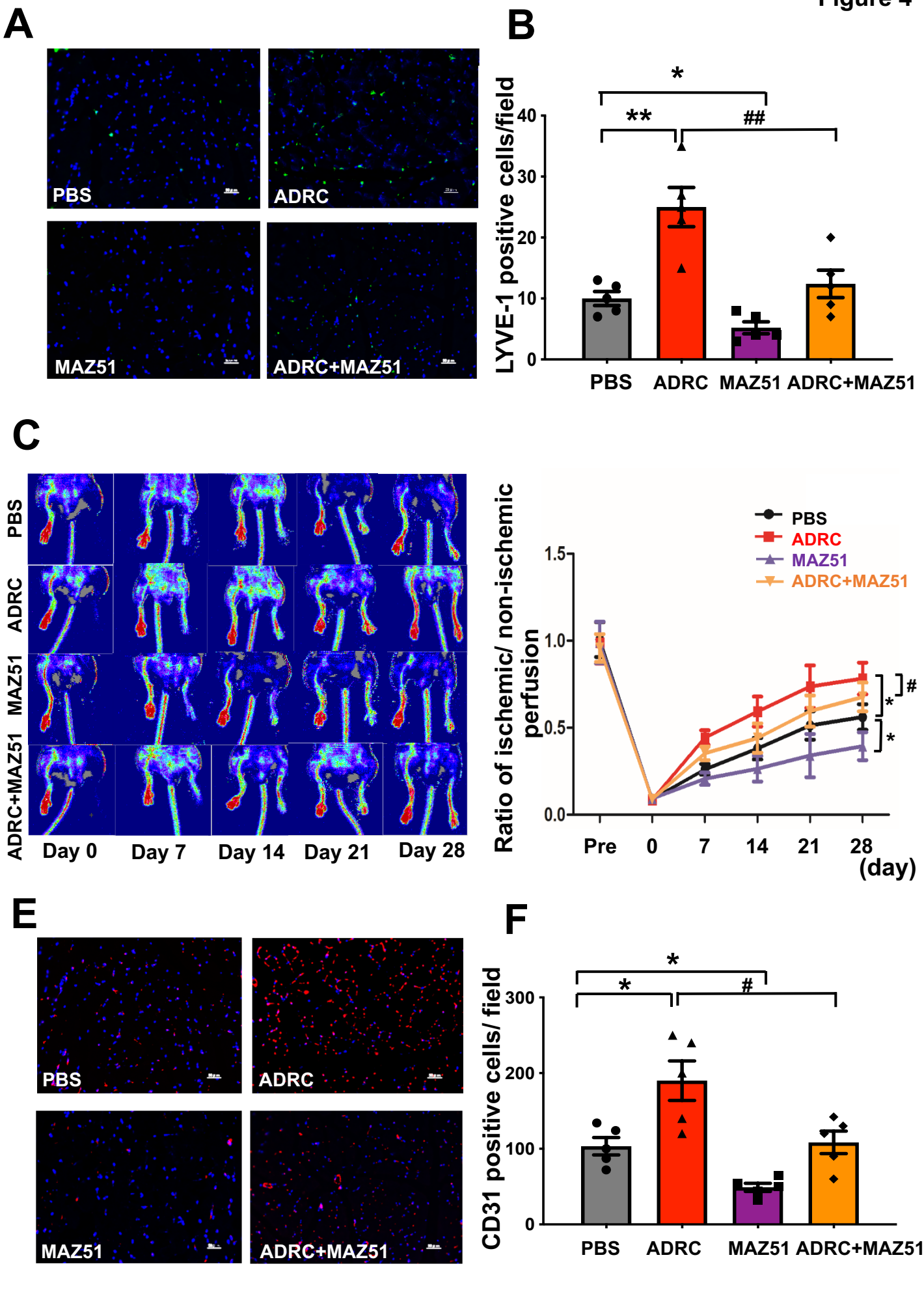
A
PBS
ADRC
MAZ51
ADRC+MAZ51
B
LYVE-1 positive cells/field
0
10
20
30
40
*
**
##
PBS
ADRC
MAZ51
ADRC+MAZ51
C
PBS
ADRC
MAZ51
ADRC+MAZ51
Day 0
Day 7
Day 14
Day 21
Day 28
Ratio of ischemic/ non-ischemic perfusion
0.0
0.5
1.0
1.5
PBS
ADRC
MAZ51
ADRC+MAZ51
*
*
#
Pre
0
7
14
21
28
(day)
E
PBS
ADRC
MAZ51
ADRC+MAZ51
F
CD31 positive cells/ field
0
100
200
300
*
*
#
PBS
ADRC
MAZ51
ADRC+MAZ51

Figure 5

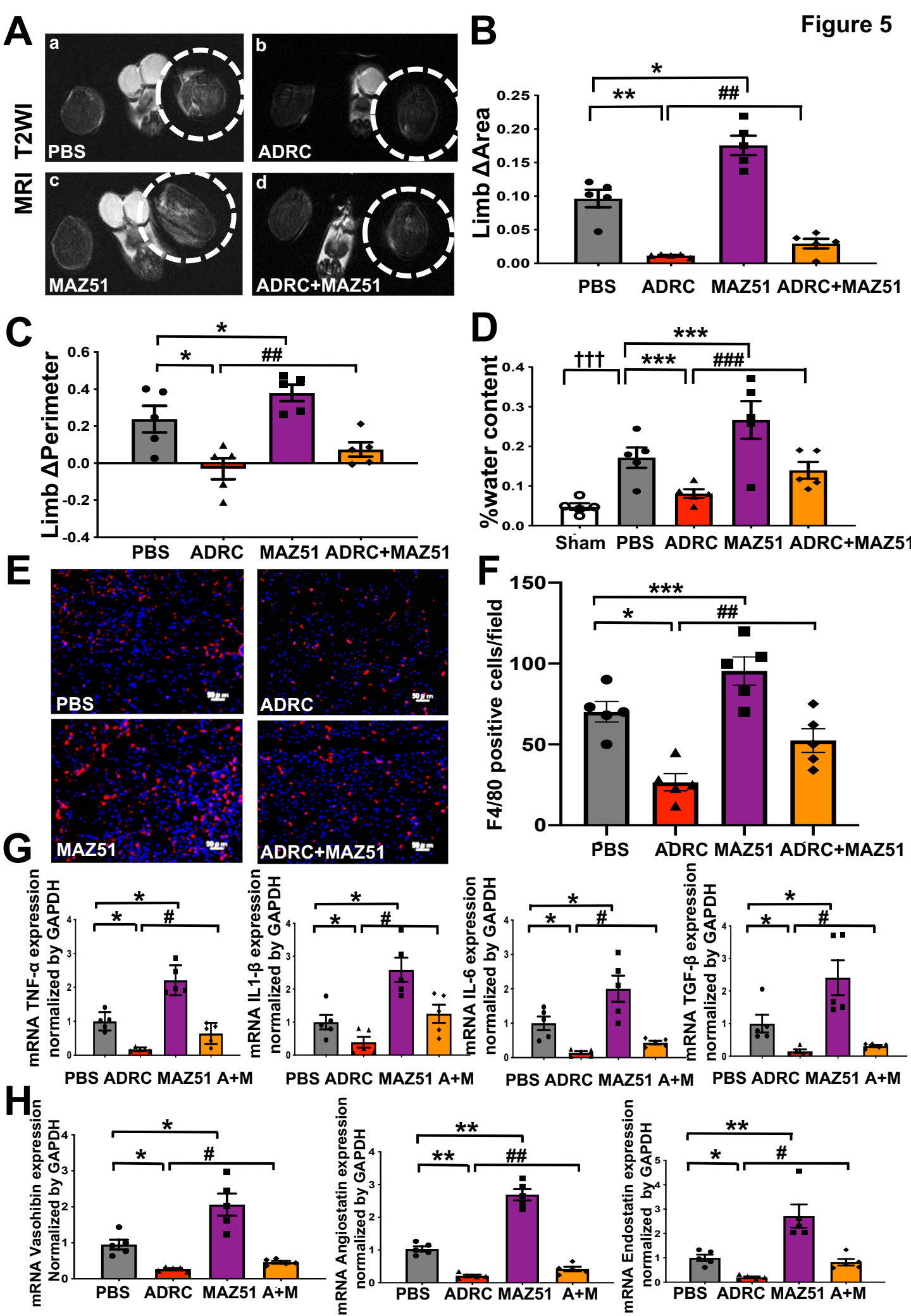
A
MRI T2WI
a
PBS
b
ADRC
c
MAZ51
d
ADRC+MAZ51
B
Limb ΔArea
0.25
0.20
0.15
0.10
0.05
0.00
*
**
##
PBS ADRC MAZ51 ADRC+MAZ51
C
Limb ΔPerimeter
0.6
0.4
0.2
0.0
-0.2
-0.4
*
*
##
PBS ADRC MAZ51 ADRC+MAZ51
D
%water content
0.4
0.3
0.2
0.1
0.0
†††
***
***
###
Sham PBS ADRC MAZ51 ADRC+MAZ51
E
PBS
ADRC
MAZ51
ADRC+MAZ51
F
F4/80 positive cells/field
150
100
50
0
***
*
##
PBS ADRC MAZ51 ADRC+MAZ51
G
mRNA TNF-α expression normalized by GAPDH
mRNA IL1-β expression normalized by GAPDH
mRNA IL-6 expression normalized by GAPDH
mRNA TGF-β expression normalized by GAPDH
*
*
#
PBS ADRC MAZ51 A+M
H
mRNA Vasohibin expression Normalized by GAPDH
mRNA Angiostatin expression normalized by GAPDH
mRNA Endostatin expression normalized by GAPDH
PBS ADRC MAZ51 A+M